

THE MECHANISM OF HEAT TRANSFER IN NUCLEATE POOL BOILING—PART II

THE HEAT FLUX-TEMPERATURE DIFFERENCE RELATION

CHI-YEH HAN* and PETER GRIFFITH†

(Received 22 September 1964 and in revised form 14 January 1965)

Abstract—The individual processes of bubble nucleation, growth and departure described in detail in Part I of this paper are used to predict the heat flux-temperature difference relation for one particular boiling experiment. The geometric idealizations made to evaluate the heat flux apply only in the isolated bubble regime. With only these idealizations, a knowledge of the surface nucleation properties, the bubble contact angle and the fluid properties is sufficient to predict the boiling performance of a surface. The comparison between the predicted and measured performance is quite good.

NOMENCLATURE

Dimensions in H, M, L, T, Θ ; The Heat Energy, Mass, Length, Time, and Temperature.

A , area of heating surface, $[L^2]$;
 D , surface characteristic length for natural convection, $[L]$;
 L , latent heat of evaporation of fluid, $[HM^{-1}]$;
 N , total number of nucleate centers on heating surface;
 N_a , total number of active nucleate centers on heating surface;
 N_i , total number of initiated nucleate centers on heating surface;
 P , pressure in the fluid outside the bubble, $[ML^{-1} T^{-2}]$;
 Q_R , heat flux received by heating surface, $[HT^{-1}]$;
 Q_P , heat flux predicted by theory, $[HT^{-1}]$;
 R , radius of bubble, $[L]$;
 R_c , radius of cavity, $[L]$;
 R_d , departure radius of bubble, $[L]$;
 S , bubble surface, $[L^2]$;

T , temperature, $[\Theta]$;
 T_b , temperature of vapor in the bubble, $[\Theta]$;
 T_{sat} , saturation temperature of fluid at system pressure, $[\Theta]$;
 T_w , wall temperature, $[\Theta]$;
 T_∞ , temperature of main body of fluid, $[\Theta]$;
 a , radius of a solid sphere, $[L]$;
 c , specific heat of fluid, $[HM^{-1} \Theta^{-1}]$;
 f , frequency of bubble generation, $[T^{-1}]$;
 g , gravity acceleration, $[LT^{-2}]$;
 h , coefficient of heat transfer from wall to the fluid, $[HT^{-1} L^{-2} \Theta^{-1}]$;
 h_v , coefficient of heat transfer from wall to vapor, $[HT^{-1} L^{-2} \Theta^{-1}]$;
 α , thermal diffusivity of fluid, $[L^2 T^{-1}]$;
 n , number of nucleate centers per unit area, $[L^{-2}]$;
 n_a , number of active nucleate centers per unit area $[L^{-2}]$;
 n_i , number of initiative nucleate centers per unit area, $[L^{-2}]$;
 p , pressure inside the bubble, $[ML^{-1} T^{-2}]$;
 q , heat flux density, $[HL^{-2} T^{-1}]$;
 t , time, $[T]$;
 t_d , departure period, $[T]$;
 t_{ub} , unbinding period, $[T]$;
 t_w , waiting period, $[T]$;
 γ , volumetric thermal expansion coefficient of fluid, $[\Theta]$;

* Senior Engineer, Research & Development Division, Royal McBee Corporation, West Hartford, Connecticut.

† Associate Professor of Mechanical Engineering, Massachusetts Institute of Technology, Cambridge, Massachusetts.

δ ,	thermal layer thickness, [L];
θ ,	$T - T_{sat}$ angle, [θ];
μ ,	coefficient of viscosity, [$MT^{-1}L^{-1}$];
ν ,	kinematic viscosity, [L^2T^{-1}];
ρ ,	density of fluid, [ML^{-3}];
ρ_v ,	density of vapor, [ML^{-3}];
σ ,	surface tension of fluid, [MT^{-2}];
φ_s ,	angle of contact in static condition;
$\tilde{\varphi}$,	dynamic contact angle at the instant of bubble departure;
φ_b ,	base factor;
φ_c ,	curvature factor;
φ_s ,	surface factor;
φ_v ,	volume factor;
Nu ,	Nusselt number;
Ra ,	Rayleigh number.

Subscripts

b_c ,	bulk convection;
cp ,	close packed condition;
d ,	departure;
nc ,	natural convection;
sat,	saturation;
ub,	unbinding;
w ,	wall, waiting.

INTRODUCTION

IT HAS NOT yet been found possible, to date, to relate the individual processes of bubble initiation, growth and departure to the boiling heat-transfer performance of a boiling surface. This paper is an account of an effort to do this. The primary purpose of any such effort is to show what information needs to be specified in order to make a boiling heat-transfer problem determinate. It will also show how the individual physical processes, on which the gross boiling phenomenon depends, combine to give the observed performance. The procedure which is used is obviously too involved to give an engineering answer in a practical boiling problem, but it can be said at this time that sufficient correlation between computed and measured results has been obtained, so that no hidden physics now remains in the process of nucleate boiling.

In Part I of this paper the individual processes of bubble initiation growth and departure were

studied and expressions obtained for these quantities. These expressions will be combined with simple geometric idealizations of the flow problem in the vicinity of the surface to give a prediction of the heat flux-temperature difference relationship.

1. HEAT-TRANSFER CORRELATION

a. *Explanation of boiling curve*

Boiling curve can be best explained by the theory of "bulk convection of the transient thermal layer". Observations show that when the wall temperature exceeds the saturation temperature of the fluid, the heat transfer increases very rapidly with the wall temperature. Many researchers have tried to explain why this occurs. The following study explains these observations by means of a so-called theory of bulk convection of the transient thermal layer, or simply bulk convection theory. When the boiling starts, the bubbles depart from the heating surface. In departing, the bubbles bring part of the layer of superheated liquid adjoining the bubble into the main body of fluid. At the same time, the cold fluid flows on to the heating surface. The heat-transfer rate for the first few moments after this process is very high due to the very high temperature gradient near the wall. After a certain time, a new thermal layer is built up, and a new bubble starts to grow. When this bubble grows to a certain size, it departs from the heating surface and a new thermal layer is brought to the main body of fluid again. By this kind of repeated transportation of thermal layer (which is technically called bulk convection), heat is transferred to the fluid from the wall. The heat-transfer rate by this process is nearly proportional to the square root of bubble generation frequency. In Fig. 1 one can see that from A to B, heat-transfer rate increases very rapidly due to the increase in $T_w - T_{sat}$ which increases the bubble generating frequency, the enthalpy content of the transient thermal layer and the density of active cavity population. At B the active cavity population has been increased to a saturation state such that the influence circle of each bubble touches one another. A further increase of $T_w - T_{sat}$ does not increase area of production of transient thermal layer, but the bubble

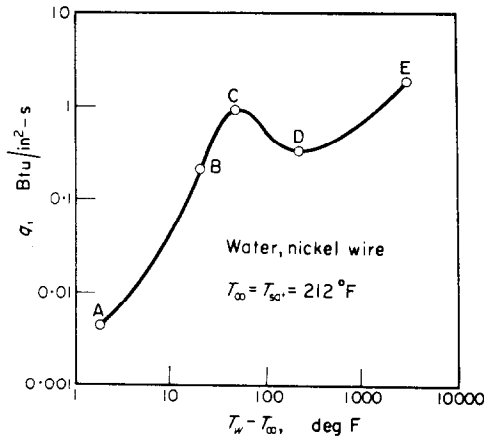


FIG. 1. Boiling curve.

frequency and enthalpy content of thermal layer continue to increase. Therefore after B the rate of increase of q is reduced. B is a point of inflexion. From B to C the bubble frequency increases until to a certain stage such that unstable and shaky vapor jets are formed. These continuous vapor columns reduce the effective area of production of transient thermal layer, such that the curve becomes concave downward. From C to D, the effective area of production of transient thermal layer decreases more rapidly than increase of the enthalpy content in the thermal layer due to increase of $T_w - T_{\text{sat}}$, therefore the curve

drops. At point D, the effective area of production of transient thermal layer has been reduced to zero, a steady and continuous blanket of vapor exists between the heating surface and main fluid. The fluid gets essentially no chance to touch the heating surface; therefore no transient thermal layer can be built up on the heating surface and the heat-transfer rate reaches to a minimum value. Bulk convection process is completely stopped at D. A further increase of $T_w - T_{\text{sat}}$ will increase heat flux again by radiation and conduction across the gap.

b. Mechanism of heat transfer

The heating surface in pool boiling is divided into two parts, the bulk convection area and the natural convection area. In the area of bulk convection, heat is assumed to be transferred into the fluid by transient conduction process. Following the departure of a bubble from the heating surface, a piece of superheated liquid is brought into the main body of the fluid. By this kind of repeated process, heat is transferred from the heating surface to the main body of the fluid. In the area of the natural convection, heat is supposed to be transferred from heating surface into the main body of fluid by the usual convection process in a continuous manner. A physical model of bulk convection mechanism is shown in Fig. 2.

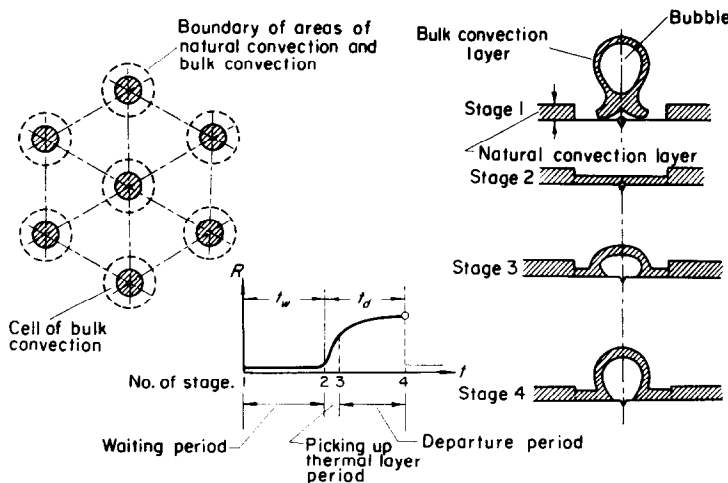


FIG. 2. Physical model of bulk convection mechanism.

At stage 1, a piece of superheated transient thermal layer is torn off from heating surface by the departing bubble, and at the same time, the cold fluid from the main body of the fluid flows on to the heating surface; after a time interval, t_w , this cold liquid layer is heated to a condition such that the tiny bubble in that cavity is able to grow laterally with a very high rate, such that a very large piece of thermal layer is picked up in a very short time interval. At stage 4, the bubble is going to depart from the heating surface which will bring the situation immediately to stage 1 again. This cyclic process furnishes a way to transfer the heat from the heating surface to the main body of the fluid.

Ideas similar to these have been expressed in several other places, too—[1, 2, 3]. In this work, however, the assumptions have been made tangible and numerical values assigned to the various process occurring.

The system which is used to evaluate the heat transfer per bubble cycle is as follows:

c. Formulation

(i) *Natural convection component.* The study of natural pool convection yields the result that natural convection heat transfer can be correlated by using two dimensionless groups, namely

$$\left. \begin{aligned} \text{The Nusselt number} \\ Nu = \frac{hD}{\rho c \alpha} \\ \text{The Rayleigh number} \\ Ra = \frac{\gamma g (T_w - T_\infty) D^3}{\alpha \nu} \end{aligned} \right\} (1)$$

For laminar range

$$\left. \begin{aligned} 10^5 < Ra < 2 \times 10^7 \\ Nu = 0.54 Ra^{1/4} \end{aligned} \right\} (a)$$

For turbulent range

$$\left. \begin{aligned} 2 \times 10^7 < Ra < 3 \times 10^{10} \\ Nu = 0.14 Ra^{1/3} \end{aligned} \right\} (b)$$

Where $D = \sqrt{A}$

$A =$ area of heating surface.

This correlation was first studied experimentally by Cryder and Finalborgo and was summarized by Fishenden and Saunders [4].

Substituting equation (1) into equation (2), and making use of the definition of heat-transfer coefficient yield

For laminar range

$$\begin{aligned} 10^5 < Ra < 2 \times 10^7 \\ q_{nc} = h (T_w - T_\infty) = 0.54 \rho c \left[\frac{\gamma g (T_w - T_\infty)^5 a^3}{D \nu} \right]^{1/4} \end{aligned} \quad (3)$$

For turbulent range

$$\begin{aligned} 2 \times 10^5 < Ra < 3 \times 10^{10} \\ q_{nc} = h (T_w - T_\infty) = 0.14 \rho c \left[\frac{\gamma g (T_w - T_\infty)^4 a^2}{\nu} \right]^{1/3} \end{aligned} \quad (4)$$

The thickness of the thermal layer of natural convection is

$$\delta_{nc} = \frac{\rho c \alpha}{q_{nc}} (T_w - T_\infty) \quad (5)$$

(ii) *Bulk convection component.* From equation (2) of Part I, one can obtain the heat transferred through unit area of heating surface to the fluid during time t as

$$\int_0^\infty (T - T_\infty) c \rho \, dx = c \rho (T_w - T_\infty) \int_0^\infty \operatorname{erfc} \frac{x}{2 \sqrt{at}} \, dx = \frac{2 \rho c (T_w - T_\infty) \delta}{\pi}$$

For this case, δ is not a constant throughout the bubble base where the transient conduction thermal layer is developing. Such a doughnut-shaped layer is illustrated in Fig. 3.

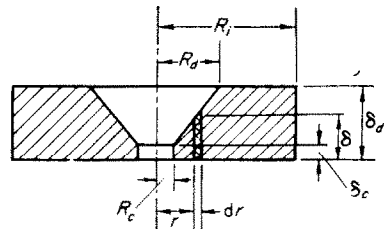


FIG. 3. Sectional view of a doughnut shaped transient thermal layer of a bulk convection cell.

For convenience in integration, the initial state is taken at the end of waiting period, so that

$$\left. \begin{aligned} \delta &= \sqrt{[\pi a (t_w + t)]} \\ \delta_c &= \sqrt{[\pi a t_w]} = \delta_w \\ \delta_d &= \sqrt{[\pi a (t_w + t_d)]} \end{aligned} \right\} \quad (6)$$

Making use of equation (5), the heat transferred into transient thermal layer, as well as in the main body of fluid beyond the transient layer during one bubble formation cycle is

$$\left. \begin{aligned} \Delta Q &= \int_{R_c}^{R_d} \frac{2 \rho c (T_w - T_\infty) \delta}{\pi} (2\pi r dr) \\ &+ \pi (R_i^2 - R_d^2) \frac{2 \rho c (T_w - T_\infty)}{\pi} \delta_d \\ &= \frac{2 \rho c (T_w - T_\infty)}{\pi} \left[\int_{R_c}^{R_i} 2\pi r \delta dr \right. \\ &\quad \left. + \pi (R_i^2 - R_d^2) \delta_d \right] \end{aligned} \right\} \quad (7)$$

where R_i is influence radius

$$R_i = 2 R_d \text{ for the isolated bubble case}$$

$$R_i < 2 R_d \text{ for the close packed case}$$

Since $R_c \ll R_d$, and δ is nearly linear in r , so equation (6) can be approximated to yield

$$\Delta Q = 2 \rho c (T_w - T_\infty) [R_i^2 \delta_d - \frac{1}{3} R_d^2 (\delta_d - \delta_c)] \quad (8)$$

If n is the number of active cavities of radius R_c per unit area of heating surface, and f is the frequency of bubble generation, then the heat-transfer rate per unit area due to bulk convection of the transient thermal layer is approximately

$$q_{BC} = nf \Delta Q = 2 \rho c (T_w - T_\infty) nf [R_i^2 \delta_d - \frac{1}{3} R_d^2 (\delta_d - \delta_c)] \quad (9)$$

(iii) *General expression for the heat transfer.* Combining equation (3) or (4) and equation (9) leads to

$$\begin{aligned} q &= q + q_{bc} = (1 - \pi \sum^n R_i^2) \\ &Nu (\rho c a / D) (T_w - T_\infty) + 2 \rho c (T_w - T_\infty) \\ &\sum^n \{ f [R_i^2 \delta_d - (R_d^2 / 3) (\delta_d - \delta_c)] \} \end{aligned} \quad (10)$$

The population density of bubbles at the close packed condition is such that the bubbles are so densely packed that the influence circle of one nucleate cell touches its neighbors; considering one half cell as indicated in Fig. 4 by shaded area, one has

$$N_{cp} = \frac{N_{cp}}{A} = \frac{\frac{1}{2}}{\frac{1}{2} (2 R_i \sqrt{3}) R_i} = \frac{1}{2 \sqrt{3} R_i^2} \quad (11)$$

where

$$R_i = 2 R_d \quad (12)$$

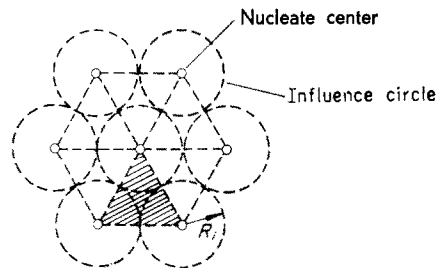


FIG. 4. Nucleate cells at close packed condition.

Equation (12) was justified by some rough experiments in which a ball of radius a was pulled up from the bottom of water tank which had a layer of chalk powder on the bottom. Observations showed that the chalk powder within a circle of radius $R_i \doteq 2a$ moved toward the center forming a vortex ring in the wake part of the ball. This vortex ring is a method of scavenging away the thermal layer within this influence circle and putting a new layer of cold liquid on the heating surface bounded by the influence circle. A sketch of this process is shown in Fig. 5.

2. EXPERIMENTAL RESULTS

Experiments were run on the same apparatus described in the first part of this paper. Measurements of heat flux, bulk temperature, wall superheat and number of active sites were made. The number of sites was determined

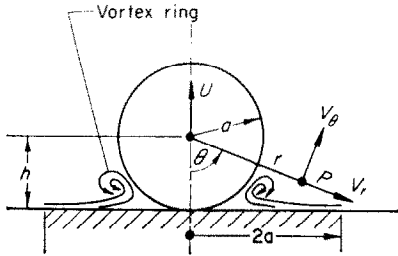


FIG. 5. Scavenging effect of a departing bubble.

by eye and the heat flux kept low enough so that counting was not difficult. As the fluid and surface were the same as in the other experiments, it was assumed the contact angles were the same also. The basic information that had to be obtained in order to allow a comparison of the calculated and experimental heat transfer-temperature difference relation is as follows:

- The number of active sites as a function of wall superheat.
- The contact angle as a function of mean bubble growth velocity.
- Fluid properties.

In calculating the heat flux-temperature difference relationship, the number of bubbles was measured experimentally. The cavity size for each bubble was computed from the relation given as equation (13) in Part I. This equation is

$$R_c = \frac{\delta (T_w - T_{sat})}{3 (T_w - T_\infty)} \left[1 \pm \sqrt{1 - \frac{12 (T_w - T_\infty) T_{sat} \sigma}{(T_w - T_{sat})^2 \delta \rho_v L}} \right] \quad (13)$$

and it has two roots. The smaller root was chosen because the greater root would necessitate having a cavity so large that it could not exist on a surface as smooth as the diamond polished surface we used. In this equation δ is δ_{nc} [equation (5)]; and $(T_w - T_{sat})$ is the temperature difference at which the site just becomes active. For this site the R_c determined in this way is a constant with increasing wall superheat. At this, the incipient condition, the waiting time t_w as given by equation (6) is infinite.

The frequency for a given cavity is determined from equation (40) of Part I which is reproduced below.

$$f = \frac{1}{t_w + t_d} \quad (14)$$

in this equation, t_w is determined from equation (12) of Part I and reproduced below as equation (15).

$$t_w = \frac{\delta^2}{\pi a} = \frac{9}{4\pi a} \left[\frac{(T_w - T_\infty) R_c}{T_w - T_{sat} [1 + (2\sigma/R_c \rho_v L)]} \right]^2 \quad (15)$$

The time it takes for a bubble to grow to departure size, t_d , is given by the bubble growth equation from Part I. This equation is (37) there and (16) here.

$$R_d - R_c = \frac{\varphi_s \varphi_c \alpha c \rho}{\varphi_v \rho_v L} \left[\frac{2(T_w - T_{sat})}{\sqrt{\pi a}} \sqrt{t_d} - \frac{T_w - T_\infty}{\delta} \frac{\delta^2}{4a} \left(\frac{4a t_d}{\delta^2} \operatorname{erf} \frac{\delta}{\sqrt{4a t_d}} + \frac{2}{\sqrt{\pi}} \frac{\sqrt{4a t_d}}{\delta} \exp[-\delta^2/4a t_d] - 2 \operatorname{erfc} \frac{\delta}{\sqrt{4a t_d}} \right) \right] + \frac{\varphi_b h_v (T_w - T_{sat})}{\varphi_v \rho_v L} t_d \quad (16)$$

This must be solved by trial and error as t_d is not yet explicitly expressed. The departure size is obtained from the Fritz relation, also reproduced from Part I equation (39) and called equation (17) here.

$$R_d = 0.4251 \varphi \sqrt{\left(\frac{2\sigma}{g(\rho - \rho_v)} \right)} \quad (17)$$

The dynamic contact angle in this equation is obtained from Fig. 16 of Part I.

The geometric idealizations used in this calculation are embodied in equation (12) and illustrated in Fig. 3. From the R_d calculated from equation (17) above and these idealizations, R_d and the various δ 's given in equation (6) can all be evaluated. When substituting in equation (10), it must be kept in mind that each different sized cavity must be computed separately, as they each have different frequencies. Using this set of equations, a comparison of the measured and calculated heat-transfer rates was made for one set of data. The calculated points are given below and the comparison given in Fig. 6. The comparison is satisfactory.

Fluid: Distilled, degassed water
 Surface: Gold, No. 8 diamond compound polished
 System pressure: 1 atm.
 T_∞ : different for each point

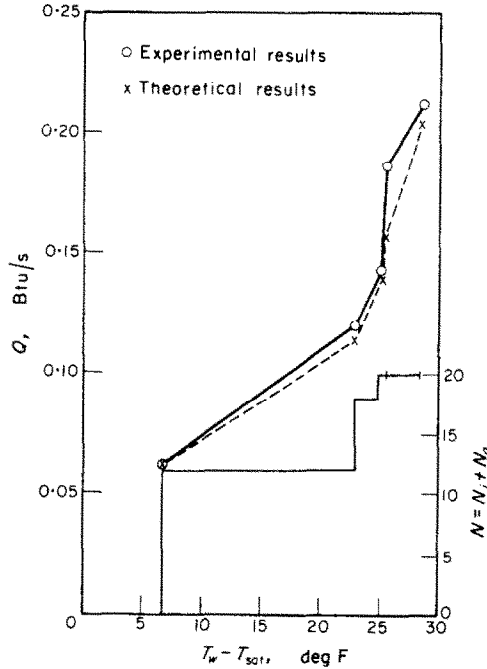


FIG. 6. Verification of bulk convection theory by Han's data.

Fluid used: Distilled degassed water

Surface: Gold layer plated on copper base, polished with No. 8 diamond compound

System pressure: $P_\infty = 1$ atm

Data point 1: $Q_R = 0.0620$ Btu/s

$T_w = 218.73^\circ\text{F}$

$T_{sat} = 212.00^\circ\text{F}$

$T_\infty = 178.56^\circ\text{F}$

$N = 12$

$N_i = 12$ of $R_c = 3.0460 \times 10^{-5}$ ft from (13), $(R_c)_{min}$ was taken as the cavity radius, since $(R_c)_{max}$ is nearly a hundred times larger than the surface texture dimension.

$N_a = 0$

$Q_P = 0.0620$ Btu/s from (10)

Data point 2: $Q_R = 0.1202$ Btu/s

$T_w = 235.09^\circ\text{F}$

$T_{sat} = 212.00^\circ\text{F}$

$$\begin{aligned}
 T_{\infty} &= 199.72^{\circ}\text{F} \\
 N &= 18 \\
 \left\{ \begin{array}{l} N_a = 12 \text{ of } R_c = 3.0460 \times 10^{-5} \text{ ft} \\ f = 69.151/\text{s} \text{ from (13), (15), (17), (16) and (14)} \\ N_i = 6 \text{ of } R_c = 0.7859 \times 10^{-5} \text{ ft} \end{array} \right. \\
 R_d &= 4.15 \times 10^{-3} \text{ ft from (17), (16)} \\
 Q_P &= 0.1142 \text{ Btu/s from (10)}
 \end{aligned}$$

Data point 3:

$$\begin{aligned}
 Q_R &= 0.1433 \text{ Btu/s} \\
 T_w &= 237.11^{\circ}\text{F} \\
 T_{\text{sat}} &= 212^{\circ}\text{F} \\
 T_{\infty} &= 201.87^{\circ}\text{F} \\
 N &= 20 \\
 \left\{ \begin{array}{l} N_a = 18 \left\{ \begin{array}{l} 12 \text{ of } R_c = 3.046 \times 10^{-5} \text{ ft} \\ f = 78.46 \text{ 1/s} \\ 6 \text{ of } R_c = 0.7859 \times 10^{-5} \text{ ft} \\ f = 53.08 \text{ 1/s} \end{array} \right. \\ N_i = 2 \text{ of } R_c = 0.7240 \times 10^{-5} \text{ ft} \end{array} \right. \\
 R_d &= 4.215 \times 10^{-3} \text{ ft} \\
 Q_P &= 0.1412 \text{ Btu/s}
 \end{aligned}$$

Data point 4:

$$\begin{aligned}
 Q_R &= 0.1866 \text{ Btu/s} \\
 T_w &= 237.61^{\circ}\text{F} \\
 T_{\text{sat}} &= 212^{\circ}\text{F} \\
 T_{\infty} &= 201.38^{\circ}\text{F} \\
 N &= 20 \\
 \left\{ \begin{array}{l} N_a = 20 \left\{ \begin{array}{l} 12 \text{ of } R_c = 3.046 \times 10^{-5} \text{ ft} \\ f = 80.72 \text{ 1/s} \\ 6 \text{ of } R_c = 0.7859 \times 10^{-5} \text{ ft} \\ f = 61.56 \text{ 1/s} \\ 2 \text{ of } R_c = 0.7240 \times 10^{-5} \text{ ft} \\ f = 6.44 \text{ 1/s} \end{array} \right. \\ N_i = 0 \end{array} \right. \\
 R_d &= 4.231 \times 10^{-3} \text{ ft} \\
 Q_P &= 0.1584 \text{ Btu/s}
 \end{aligned}$$

Data point 5:

$$\begin{aligned}
 Q_R &= 0.2157 \text{ Btu/s} \\
 T_w &= 240.65^{\circ}\text{F} \\
 T_{\text{sat}} &= 212.00^{\circ}\text{F} \\
 T_{\infty} &= 200.53^{\circ}\text{F} \\
 N &= 20 \\
 \left\{ \begin{array}{l} N_a = 20 \left\{ \begin{array}{l} 12 \text{ of } R_c = 3.046 \times 10^{-5} \text{ ft} \\ f = 88.03 \text{ 1/s} \\ 6 \text{ of } R_c = 0.7859 \times 10^{-5} \text{ ft} \\ f = 87.06 \text{ 1/s} \\ 2 \text{ of } R_c = 0.7240 \times 10^{-5} \text{ ft} \\ f = 78.60 \text{ 1/s} \end{array} \right. \\ N_i = 0 \end{array} \right. \\
 R_d &= 4.322 \times 10^{-3} \text{ ft} \\
 Q_P &= 0.2056 \text{ Btu/s}
 \end{aligned}$$

3. DISCUSSION

In the preceding paper it has been shown possible to predict the q vs $T_w - T_{\text{sat}}$ relation for one particular geometry in the isolated bubble region. An extraordinary amount of information about the surface was needed to do this. In a practical problem this information hardly exists, so where do we go from here? First we can now design meaningful experiments as we know all the variables. Second, these experiments show the following:

- (a) More systematic experimentation needs to be done to determine how invariant the surface variables of contact angle and nucleation properties are. This should be done on industrial type apparatus rather than on laboratory size experiments.
- (b) It should be possible to develop highly simplified q vs $(T_w - T_{\text{sat}})$ relations in which the invariant surface properties appeared as a curve of arbitrary shape. This would be an improvement over assuming a constant power on $(T_w - T_{\text{sat}})$ in a boiling correlation. It would be desirable if the independent variables like sub-cooling, pressure and velocity were included in the functional relations.
- (c) More information needs to be obtained on the significance of small differences in handling procedure from batch to batch of typical boiling surfaces. This would fix the limit of significance of any boiling correlation.

4. CONCLUSIONS

- (a) Viscosity does not enter directly into the boiling process but only in its effect on bubble departure and contact angle variations.
- (b) Surface conditions, through nucleation properties and contact angles, explicitly affect the boiling process.
- (c) The complications of the boiling process are reflected in the complications in the boiling data.
- (d) A bubble departure criterion must be specified in order that the boiling process be determinate.
- (e) The heat-transfer geometry, as affected by bubble packing, size and shape must be specified to make the boiling heat-transfer process determinate.

REFERENCES

1. W. M. ROHSENOW, A method of correlating heat-transfer data for surface boiling of liquids, *Trans. Amer. Soc. Mech. Engrs* **74**, 969-976 (1962).
2. K. FORSTER and R. GRIEF, *J. Heat Transfer* **81**, 43-53 (1959).
3. N. ZUBER, Nucleate boiling—Part I. Similarity with natural convection. Report No. 61 GL 166, General Electric (August, 1961).
4. M. FISHENDEN and O. A. SAUNDERS, *Heat Transfer*. Oxford University Press, London (February, 1950).
5. CHI-YEH HAN, The mechanism of heat transfer in nucleate pool boiling, Sc.D. Thesis, M.I.T. (1962).

Résumé—Les processus individuels de la germination des bulles, de leur croissance et de leur détachement qui ont été décrits en détail dans la 1ère partie de cet article sont utilisés pour prévoir la relation entre le flux de chaleur et la différence de température pour une expérience particulière d'ébullition.

Les idéalizations géométriques faites pour évaluer le flux de chaleur s'appliquent seulement dans le régime avec bulle isolée. Avec seulement ces idéalizations, une connaissance des propriétés de germination de la surface, de l'angle de contact de la bulle et des propriétés du fluide est suffisante pour prévoir les performances d'une surface pour l'ébullition. La comparaison entre les performances prévues et mesurées est tout à fait bonne.

Zusammenfassung—Die einzelnen Vorgänge des Entstehens von Blasen, ihres Anwachsens und Ablösens, die im einzelnen in Teil I dieser Arbeit beschrieben wurden, werden zur Vorhersage der Beziehung zwischen Wärmestromdichte und Temperaturdifferenz für einen besonderen Siederversuch verwendet. Die geometrischen Vereinfachungen wurden getroffen, um die Wärmestromdichte nur für den Bereich der Einzelblasen abzuschätzen. Mit ausschliesslich diesen Vereinfachungen genügt das Kennen der Eigenschaften der Keimstellen an der Oberfläche, des Blasenrandwinkels und der Stoffwerte der Flüssigkeit, um die Siedeleistung einer Oberfläche vorherzusagen. Der Vergleich zwischen der vorhergesagten und der gemessenen Leistung ist recht gut.

Аннотация—Представления о процессах образования, роста и отрыва пузырьков, подробно описанные в Части I этой статьи, использованы здесь для расчета соотношения между тепловым потоком и разностью температур для одного конкретного опыта по кипению. Геометрическая идеализация позволила рассчитать тепловой поток применительно только к изолированному пузырьковому режиму. Только при такой идеализации для описания кипения на какой-либо поверхности достаточно знать свойства этой поверхности, как места зарождения пузырьков, краевой угол пузырька и свойства жидкости. Сравнение расчетных и опытных данных дает хороший результат.